ISSN 0388-9394

Tech. Bull.
Trop. Agr. Res.
Center, Japan
No. 26

Technical Bulletin

of

the Tropical Agriculture Research Center

No. 26 1989

ANALYSIS OF LIGHT CLIMATE UNDER THE CANOPY OF A MAN-MADE FOREST IN THE TROPICS

YOICHI KANAZAWA, SHOZO NAKAMURA

and

ROBERTO V. DALMACIO

TROPICAL AGRICULTURE RESEARCH CENTER
MINISTRY OF AGRICULTURE, FORESTRY AND FISHERIES, JAPAN

Tropical Agriculture Research Center
Ministry of Agriculture, Forestry and Fisheries
Ohwashi, Tsukuba, Ibaraki 305, Japan

Technical Bulletin of the Tropical Agriculture Research Center No. 26

ANALYSIS OF LIGHT CLIMATE UNDER THE CANOPY OF A MAN-MADE FOREST IN THE TROPICS

Yoichi KANAZAWA*,**, Shozo NAKAMURA***
and
Roberto V. DALMACIO****

1989

* Tropical Agriculture Research Center, Tsukuba, Ibaraki 305, Japan
** Present address: Hokkaido Research Center, Forestry and Forest Products Research Institute, Sapporo 004, Japan
*** Kyushu Research Center, Ditto, Kumamoto 860, Japan
**** College of Forestry, University of the Philippines, College, Laguna 3720, Philippines

Tropical Agriculture Research Center
Ministry of Agriculture, Forestry and Fisheries
Ohwashi, Tsukuba, Ibaraki 305, Japan

Printed by Foundation Norin Kosaikai

ABSTRACT

KANAZAWA, Y., NAKAMURA, S. and DALMACIO, R. V., 1989, Analysis of light climate under the canopy of a man-made forest in the tropics.

Tech. Bull., Trop. Agr. Res. Center, Japan, No. 26

The light climate under the forest canopy was analyzed from the viewpoint of multistoried agroforestry systems. Illuminance under the tree crown was proportional to that in the open within a certain range, but it tended to be stable or rather to decrease with increasing illuminance in the open over this range. This phenomenon seemed to be due to the lack of differentiation between the direct and diffuse fractions of sunlight. Based on model experiments, only the diffuse fraction appears to affect directly the radiation under the shade, and the radiation climate could be analysed by two models simulating diffuse sunlight. The opening proportion in the canopy visualized by the hemispherical photographs was closely related to the diffuse radiation under the canopy. Solar radiation on the ground of *Acacia auriculiformis* A. CUNN. ex BENTH. stands was analysed by hemispherical photography and actual radiation measurements. The relationship between the stand structure and radiation reaching the ground for a given period could be formulated and diagrammatically illustrated based on the analysis. The results obtained for *A. auriculiformis* stands were compared with those obtained in preliminary studies of actual multistoried systems consisting of coconut palms and other agricultural crops.

Index words: light climate under the canopy, multistoried agroforestry system, direct radiation, diffuse radiation

CONTENTS

I. Introduction

In recent years, overcutting of fuel wood and saw timber and short rotation of shifting cultivation have become common in the tropical and subtropical regions. These practices have resulted not only in the reduction of the forest area but also in the destruction of the local ecosystems including arable land by natural disasters such as soil erosion, frequent flooding and critical drought[8)18)]. Under these conditions, it is natural that various projects of reforestation or afforestation have been planned and implemented in these regions, so far.

"Agroforestry" can be considered to be one of the attempts to establish forests. Agroforestry is a system which aims originally at higher land utilization through the combined effect of production of agricultural crops and land conservation by forests through a temporal or permanent and spatial combination of agriculture and forestry[8)18)]. In some agroforestry systems, forestry is combined with animal husbandry instead of agriculture. From the social and economic viewpoints, this system may induce farmers to abandon shifting cultivation practices and to become fixed on the land when arable land is provided. However many problems must be solved for the effective implementation of agroforestry systems. Apart from social and economical aspects, studies on agroforestry are being undertaken from the technical and scientific standpoints.

Of the various types of agroforestry systems, the mixed farming system including agricultural and silvicultural crops may be the most popular one presently in Southeast Asia. This system often leads to a multistoried structure: trees and agricultural crops form the upper and lower layers, respectively. In this system, the trees in the upper layer have a great influence on the light climate of the lower crops. Since the light factor affects strongly the growth of the crops, the analysis of the relationship between trees and light conditions in the lower layers is essential for the development of techniques for growth control of the lower crops. Therefore, in this report, first of all, we concentrated our studies on the light climate under the canopy, and attempted to analyze theoretically and practically the relationship between the stand structure and the light or the radiation coming through the canopy. This detailed analysis will undoubtedly contribute significantly to practical applications.

This work was carried out in 1986 and 1987 while Y. KANAZAWA and S. NAKAMURA were staying at the College of Forestry, University of the Philippines, as long-term and short-term visiting scientists, respectively, dispatched by Tropical Agriculture Research Center, Ministry of Agriculture, Forestry and Fisheries.

We thank Dr. Celso B. LANTICAN, former Dean of the College of Forestry, University of the Philippines, for his guidance and help during this work, Dr. Fumio IWATA, former Director of the Second Research Division of the Tropical Agriculture Research Center, for his suggestions, and Dr. Sumihiko ASAKAWA, former Director of the Silviculture Division of the Forestry and Forest Products Research Institute, for his valuable advice and assistance. Thanks are also due to Messrs. Hitoshi KATO, chief adviser, and Tsutomu HANDA, former team leader, and other Japanese experts of the Pantabangan Reforestation Project Team of JICA, for their cooperation in giving the opportunity to use the project site and for their support.

II. Illuminance measured under several tree crowns

As a method to assess the light conditions inside and under a canopy, the relative illuminance (RI) has been used so far in many reports. The RI is the percentage of the illuminance inside the canopy to that outside. Here, as a first step for analyzing the light climate under the canopy, the illuminances under the crown of several trees and in the open were measured at the campus of the College of Forestry, University of the Philippines at Los Baños, and the values of RI and the absolute illuminance were compared.

1. Materials and methods

Two large leaf mahogany (*Swietenia macrophylla* KING) trees and one tree each of teak (*Tectona grandis* L.) and balitbitan (*Cynometra ramiflora* L.) were selected in the garden in front of the administration building of the College of Forestry. Several measurement points were positioned horizontally under each tree crown. The measurements were carried out during seven days between late March and early April in 1986 using the T-1H type illuminance meter of Minolta Camera Ltd. Illuminances both just above the measurement point and in the open were measured simultaneously around noon. Several dimensions of the selected trees are shown in Table 1.

Table 1. Tree parameters

Species		DBH (cm)	Height (m)	Crown width (m × m)	Crown height (m)
Large leaf mahogany 1 (*Swietenia macrophylla* KING)		30.3	11.0	11.2 × 5.2	3.2
- Ditto -	2	4.2	3.9	0.6 × 0.6	1.9
Teak (*Tectona grandis* L.)		94.4	25.0	12.9 × 14.3	4.2
Balitbitan (*Cynometra ramiflora* L.)		13.4[a)] 7.3	5.5	6.9 × 7.7	2.2

a) Two stems

2. Results and discussion

The measurements were carried out on clear, slightly cloudy and totally cloudy days. Typical relationships of illuminance between the open and under the crown are shown in Fig. 1. The illuminance under the crown was roughly proportional to that in the open within a certain range although some deviations were observed. However, when the illuminance in the open exceeded the proportional range, that under the crown rather decreased. The highest illuminance under the crown was observed on slightly cloudy days. On the other hand, the illuminance under the crown tended to decrease on perfectly clear days without clouds. The highest illuminance of 100klux

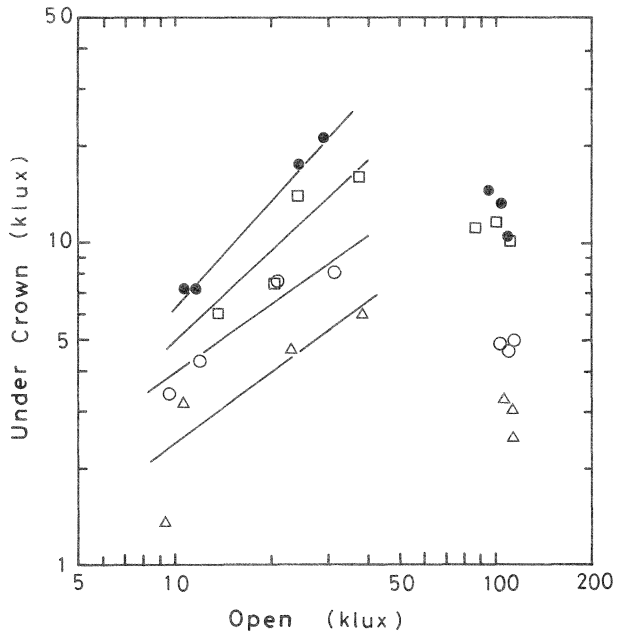

Fig. 1. Relationship of illuminance between the open and under the crown of four trees, i.e. two large leaf mahogany (*Swietenia macrophylla* KING) trees (1: open circle) (2: solid circle), one teak tree (*Tectona grandis* L.) (open square), and one balitbitan tree (*Cynometra ramiflora* L.) (open triangle). The measurement was carried out under various weather conditions. Regression lines were drawn for less than 50 klux in the open.

was recorded in the open, when it was clear with woolly clouds.

The phenomenon described above was already reported by several authors[17)23)25)], among which SASAKI & MORI[23)] recognized that, the illuminance on the forest floor increased with the increasing illuminance outside, but it tended to remain stable when the outside illuminance exceeded a certain value. Although the irradiance differs from the illuminance, ANDERSON[4)] observed minor fluctuations in the irradiance under the shade. Based on their and our results the following conclusion may be drawn. The light in the open consists of the light coming directly from the sun (direct sunlight fraction) and that from the sky (diffuse light fraction), whereas the light coming through the crown is only the diffuse light, except for sunflecks. Accordingly, the light under the shade is closely related to the total diffuse light from the sky. It seems obvious that the total diffuse light increases by the scattering and reflection of direct sunlight by clouds on a cloudy day, as compared with a cloudless day. This explanation accounts for the fact that the highest illuminance under the crown was recorded on clear days with woolly clouds.

As noticed above, two main fractions of light, direct and diffuse light, should be separated when analyzing the light climate inside and under the canopy[2)3)]. The RI is defined as the illumination percentage inside the canopy to that outside of the canopy. If the calculation is made including the direct sunlight fraction, RI would decrease

even when the absolute illuminance inside the canopy shows a constant level. The concept of RI is originally based on the assumption that the absolute illuminance at the measurement point would be proportional to that in the open. Therefore, the direct sunlight fraction should be excluded for the calculation of RI. MONSI & SAEKI[16] already showed that the measurements should be made on cloudy days for the calculation of RI, suggesting that only the diffuse light is required for the RI calculation.

III. Model experiments of diffuse radiation

In the preceding chapter, we concluded that the illuminance under the shade depends on the total diffuse light from the sky, and generally remains at a constant level even when the illuminance in the open exceeds a certain range. However, the illuminance is the visible unit of radiation seen by the human eye, and it does not necessarily follow that its wavelength corresponds to the active wavelength for photosynthesis or heat balance in plants. It is preferable to use the irradiance for the analysis of the relationship between solar radiation and plant growth. Here in this chapter, therefore, the diffuse radiation under the shade was investigated again in terms of irradiance and photon flux of photosynthetically active radiation (PAR) using some models.

1. Methods

Silicon energy sensors (QS and ES type of Delta-T devices Ltd.) were used for the measurements. The former is a quantum sensor measuring the photon flux density in the 400 to 700 nm wavelength range, i.e. PAR. On the other hand, the latter measures the radiant flux density of wavelengths ranging between 400 and 1,000 nm.

1) Experiment I

To avoid interferences around the sensor as much as possible, the sensor was set on the rooftop of a building. As shown in Fig. 2, a disc painted black was put above the sensor to obtain the opening angle (θ) above the horizon. For opening angles from 10° to 60°, a total of six discs were prepared for every 10°. For each angle, the photon flux density and the radiant flux density were recorded. The record in the open was obtained simultaneously. The shading naturally eliminated the direct solar radiation and consequently only the diffuse one could be measured.

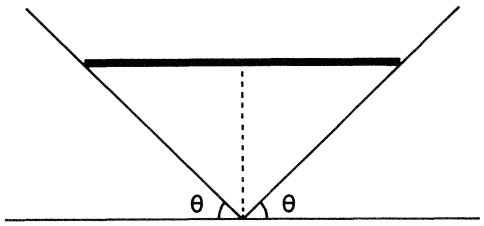

Fig. 2. Illustration of Experiment I. Solar radiation comes from the opening angle between 0° and θ.

2) Experiment II

This experiment was carried out on the same rooftop as in Experiment I. However, the opening angle was set from the zenith in contrast to Experiment I (Fig. 3). In this experiment, the sensor was put inside a cylinder and the opening angle was adjusted based on the size of the punched hole on the plate placed on top of the cylinder. The inside of the cylinder and plate was painted black to prevent reflection. The opening

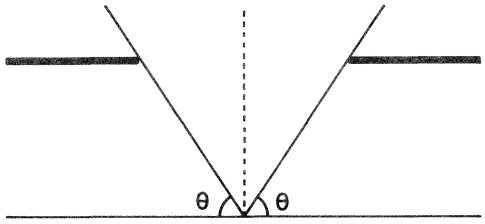

Fig. 3. Illustration of Experiment II. The angle 0° to θ was shaded from the sun.

angles ranged from 30° to 80° and changes were made at every 10°. In this experiment, the diffuse radiation could be obtained by subtracting the values of the shading treatment from those in the open. Experiments I and II were carried out around noon between late January and early February in 1987.

3) Two models for diffuse illuminance

Two models simulate the diffuse illuminance. We attempted to apply these models to the results of this experiment, altough the definition of illuminance is different from that of irradiance and photon flux. An explanation of these modles should be briefly given here before discussion.

One model is based on an empirical equation of luminance distribution in the sky proposed by MOON & SPENCER (1942) (after ANDERSON[2]). They expressed the luminance at a point in the sky ($L\theta$) as

$$L_\theta = \frac{1}{3} L_Z (1 + 2\sin\theta),$$

where θ is the angle of altitude of the point and L_Z the luminance at the zenith, and the radius of the radiating hemispherical shell is dealt with as unity. From this equation and the cosine law, the luminous flux coming from an annulus at θ in the sky to a point on the horizontal surface ($D\theta_1$) can be calculated as

$$D_{\theta 1} = \frac{1}{3} L'_Z (1 + 2\sin\theta) \cdot 2\pi \sin\theta \cos\theta = \frac{2}{3} L'_Z \pi (\sin\theta + 2\sin^2\theta)\cos\theta \cdots\cdots 1,$$

where L'_Z refers to a uni-directional flux from the zenith with L_Z. By integration, the total luninous flux from altitudes 0° and θ becomes

$$\int_0^\theta D_{\theta 1} \mathrm{d}\theta = \frac{2}{3} L'_Z \pi \int_0^\theta (\sin\theta + 2\sin^2\theta)\cos\theta \,\mathrm{d}\theta = L'_Z \pi \left(\frac{1}{3}\sin^2\theta + \frac{4}{9}\sin^3\theta\right).$$

If L'_Z=1 and the radius is $1/\pi$, this equation agrees with that proposed by WALSH described by ANDERSON[2]. The condition expressed by this equation is designated as the standard overcast sky (SOC)[2)17)].

In another model, the luminous flux from all points in the sky is assumed to be uniform. This condition is known as the uniform overcast sky (UOC)[17)]. From the cosine law, the diffuse illuminance from an annulus at θ($D\theta_2$) is calculated as

$$D_{\theta 2} = L'_Z \sin\theta \cdot 2\pi \cos\theta = 2 L'_Z \pi \sin\theta \cos\theta \cdots\cdots 2.$$

Then, the total luminous flux from the opening between 0° and θ would be

$$\int_0^{\theta} D_{\theta 2}\,\mathrm{d}\theta = L'_z \pi \int_0^{\theta} 2\sin\theta\cos\theta\,\mathrm{d}\theta = L'_z \pi \sin^2\theta$$

Here, we designate the former as the SOC model and the latter as the UOC model. Fig. 4 shows both patterns based on these models of diffuse illuminance coming from the region between altitudinal angles 0° and θ.

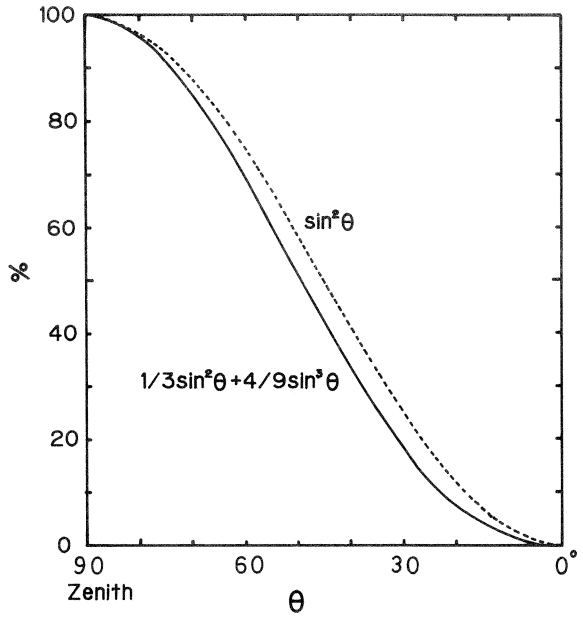

Fig. 4. Relative diffuse illuminance between 0° and θ above the horizon based on two models, i.e. standard overcast sky (SOC) and uniform overcast sky (UOC). The SOC and UOC are given as $1/3\sin^2\theta+4/9\sin^3\theta$ and $\sin^2\theta$, respectively.

2. Results and discussion

1) Experiment I

The results of the photon flux density are shown in Figs. 5–8. As in the case of the illuminance, stable values under the shade were also observed for each opening angle, and they increased with the increase of the opening angle. A typical example was seen on Jan. 29 (Fig. 5). However, there were differences in the photon flux density on the different days even for the same opening angle. On some days clouds passed the sun very quickly and frequently. Minor fluctuations were observed in the photon flux density under the shade even under such weather conditions, forming a striking contrast with those in the open as shown in Photo. 1. Irradiance under the shade was also practically stable in spite of the fluctuations in the open as in the photon flux density, when θ was maintained a fixed altitudinal degree (Fig. 9). This fact indicates that the radiation under the shade depends on the total diffuse radiation from the sky

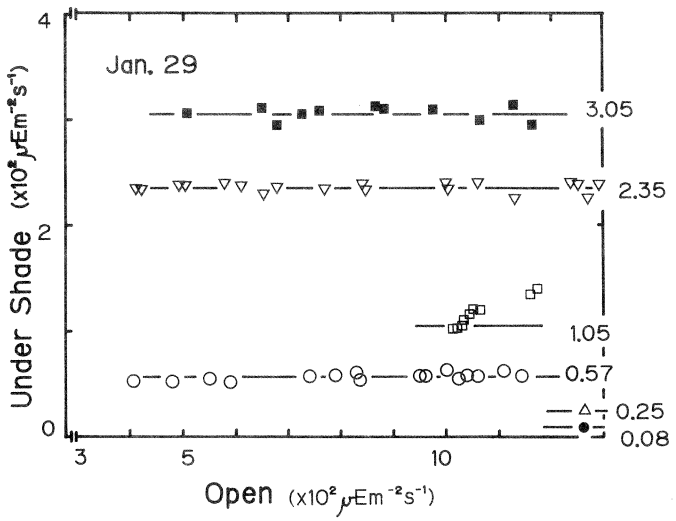

Fig. 5. Photon flux densities in the open and under the shade in Experiment I measured on Jan. 29. Opening angles (θ) were 10° (solid circle), 20° (open triangle), 30° (open circle), 40° (open square), 50° (reverse open triangle), and 60° (solid square). Solid lines and figures refer to the average for each angle.

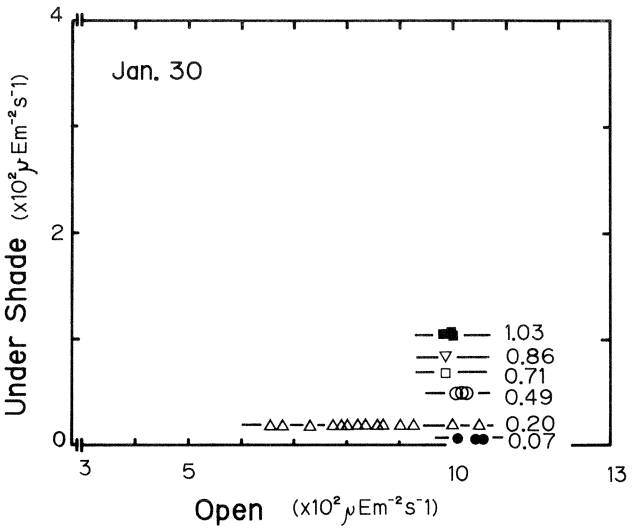

Fig. 6. Experiment I: results of measurements performed on Jan. 30. Symbols and figures are the same as in Fig. 5.

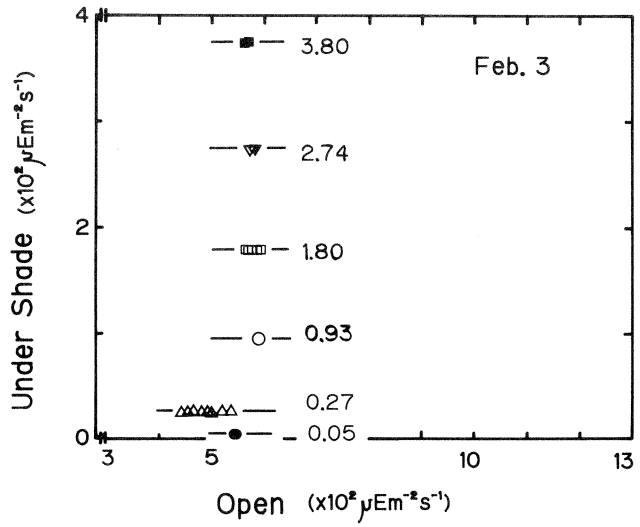

Fig. 7. Experiment I: results of measurements performed on Feb. 3.

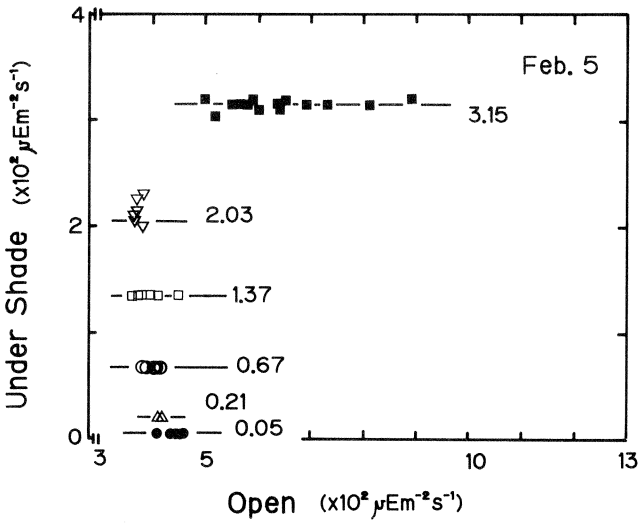

Fig. 8. Experiment I: results of measurements performed on Feb. 5.

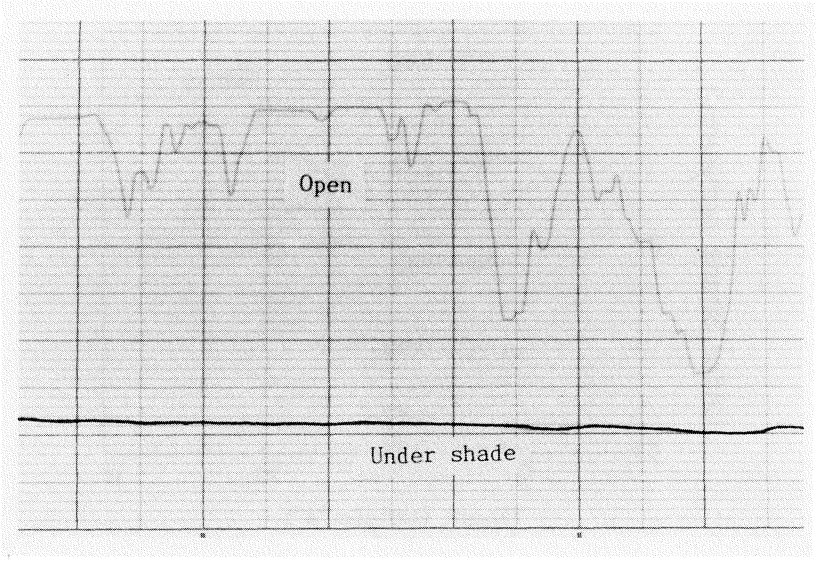

Photo.1. Example of recording of photon flux density of PAR which fluctuates in the open and is stable under the shade.

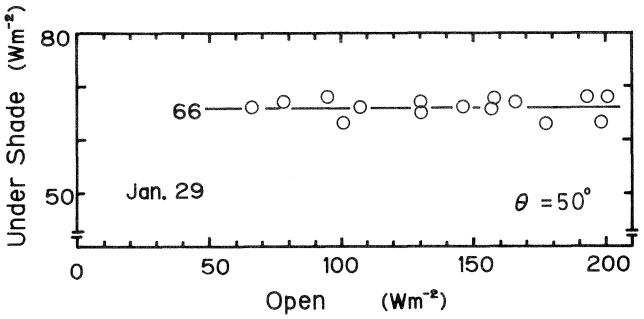

Fig. 9. Example of stable radiant flux density under the shade despite fluctuation of values in the open.

whose fluctuations are minor compared with the direct one.

In Fig. 10 the results are presented in relation to the SOC model. A higher correlation was found between the photon flux density at an opening angle θ and $1/3\sin^2\theta+4/9\sin^3\theta$. Similar results were obtained for values of irradiance from 400 to 1,000 nm (Fig. 11). This close relationship indicates the validity of the application of diffuse illuminance models to the diffuse radiation. Difference in the gradient of the regression line as shown in Figs. 10 and 11 may be due to the difference in the diffuse radiation from the whole sky.

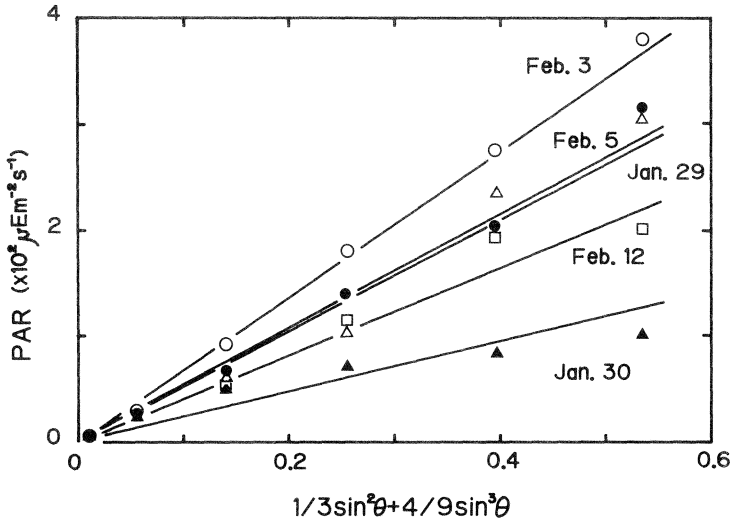

Fig. 10. Linear regressions between photon flux density of PAR and $1/3\sin^2\theta+4/9\sin^3\theta$ (SOC model) in Experiment I. Symbols are assigned to the measurement dates; open circle (Feb. 3), solid circle (Feb. 5), open triangle (Jan. 29), open square (Feb. 12), and solid triangle (Jan. 30).

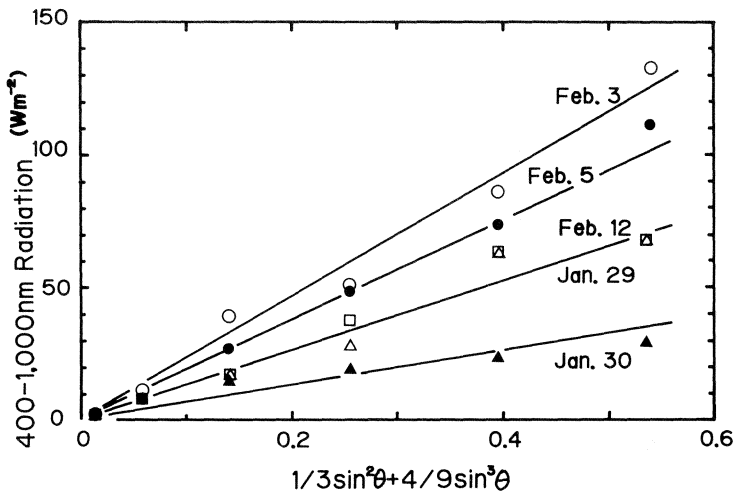

Fig. 11. Linear regressions between radiant flux density (400-1,000 nm) and $1/3\sin^2\theta+4/9\sin^3\theta$ (SOC model) in Experiment I. Symbols are the same as in Fig. 10.

2) Experiment II

In this experiment, only two measurements could be obtained on cloudy days to avoid the direct radiation when the θ was low. As shown in Figs. 12 and 13, there was a close correlation between the subtracted values and $1/3\sin^2\theta+4/9\sin^3\theta$, showing the good agreement of the measurement values with the diffuse illuminance models.

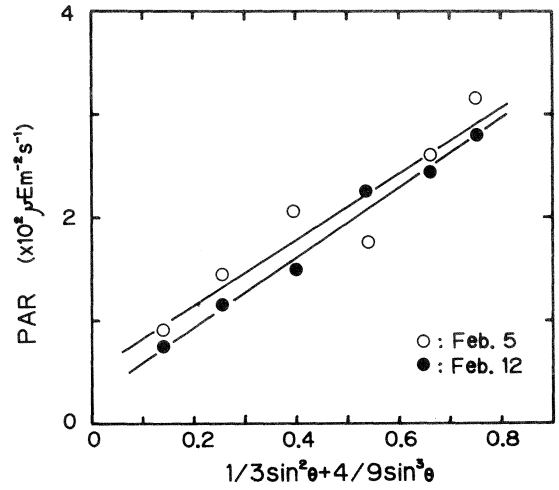

Fig. 12. Results of Experiment II (photon flux density of PAR) using the SOC model.

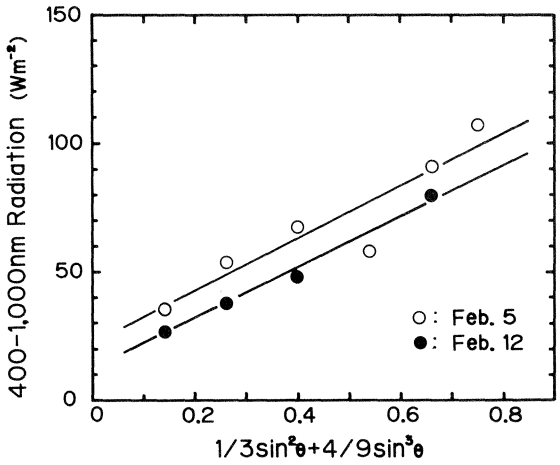

Fig. 13. Results of Experiment II (radiant flux density) using the SOC model.

3) Application of two diffuse illuminance models to the radiation under various weather conditions

The fitness of the two models for the actual measurements is presented in Table 2 in terms of the correlation coefficient of the linear regression. The coefficient of the SOC model seems to be only slightly higher than that of the UOC model. Typical SOC and UOC could not be observed during the experiment. Nevertheless, the diffuse radiation from the sky could be approximated by the illuminance models despite differences in the cloud conditions. This fact implies that both models can be practically used for the simulation of the diffuse radiation, taking the measurement errors into account. The difference between the two models must be considered depending on the purpose.

Table 2. Correlation coefficients of the relationship between diffuse radiation coming from 0° to θ above the horizon, and angle distribution in the models

Date of measurement/Model			SOC[a] $1/3\sin^2\theta+4/9\sin^3\theta$	UOC[b] $\sin^2\theta$
Experiment I	Jan. 29	a[d]	0.9889	0.9780
		b[e]	0.9723	0.9548
	Jan. 30	a	0.9723	0.9869
		b	0.9735	0.9902
	Feb. 3	a	0.9997	0.9965
		b	0.9945	0.9908
	Feb. 5	a	0.9965	0.9889
		b	0.9974	0.9904
	Feb. 12	a	0.9789	0.9826
		b	0.9823	0.9858
Experiment II	Feb. 5	a	0.9345	0.9307
		b	0.9274	0.9202
	Feb. 12	a	0.9921	0.9918
		b[g]	0.9950	0.9887

a) Standard overcast sky
b) Uniform overcast sky
c) Obscured from the zenith to the angle ($90°-\theta$) (Fig. 2)
d) Photon flux density of PAR (400–700 nm)
e) Radiant flux density (400–1,000 nm)
f) Estimated by the difference between 90° and ($90°-\theta$) from the zenith (Fig. 3)
g) Only four samples

4) Factors affecting diffuse radiation under the canopy

As suggested by the above discussion, the diffuse radiation under the canopy can be affected by several factors: total diffuse radiation from the sky which fluctuates with time and the weather conditions, and characteristics of shading objects, i.e. their size and position in the sky. In other words, openings in the canopy can be responsible for the diffuse radiation reaching the forest floor. Aside from the absolute value of the radiation, the use of hemispherical photographs seems to be suitable for the evaluation of the openings in the canopy. In the next chapter, we will analyze the relationship between the relative diffuse radiation and the openings in the canopy by using hemispherical photographs.

IV. Relationship between relative diffuse radiation and the opening proportion in hemispherical photographs

To assess the light climate under the canopy, the use of hemispherical photographs has been attempted so far. Some reports revealed a close correlation between the magnitude of the openings and the RI[6)26)27)]. For the assessment a more detailed treatment of the photograph was also suggested in other reports[2)7)9)11)12)15)24)]. The hemispherical image taken by the fisheye lens is characterized by the direct proportion of the radius to the angle from the zenith although some correction is needed. Based on this characteristic, the relative diffuse radiation under the canopy will be theoretically analyzed in this chapter.

The hemispherical photographs used here were taken at several *Acacia auriculiformis* A. CUNN. ex BENTH. stands in Carranglan, Nueva Ecija. The procedure of photography and interpretation of the hemispherical image will be described in the next chapter.

1. Discussion

1) Theoretical considerations about diffuse radiation coming through openings in the canopy

Based on equations 1 and 2 described in the preceding chapter and on the equation $\delta \equiv 90° - \theta$, the diffuse radiation coming from a zenith angle (δ) is calculated for both models as follows:

$$D_{\delta 1} = \frac{2}{3} L'_Z \pi (\cos\delta + 2\cos^2\delta)\sin\delta \quad \text{(SOC model)} \cdots\cdots 3$$

or

$$D_{\delta 2} = 2 L'_Z \pi \cos\delta \sin\delta \quad \text{(UOC model)} \cdots\cdots 4.$$

where $D_{\delta 1}$ and $D_{\delta 2}$ are the diffuse radiation for the SOC and the UOC model, respectively. Their pattern in relation to δ is shown in Fig. 14. When, in the circular hemispherical image, the proportion of the unshaded arc on the circumference at a given angle δ is given as $k(\delta)$, D_r as the diffuse radiation coming from δ can be calculated in both models as

$$D_{r1} = D_{\delta 1} \cdot k(\delta) \cdots\cdots 5$$

and

$$D_{r2} = D_{\delta 2} \cdot k(\delta) \cdots\cdots 6,$$

respectively. The subscripts 1 and 2 refer to the SOC and the UOC model, respectively. Dividing the integrated value obtained in equation 5 or 6 from 0° to 90° by that in equation 3 or 4, the relative diffuse radiation RD_1 or RD_2 can be theoretically calculated, i.e.

$$RD_1 = \frac{\int_0^{\pi/2} D_{\delta 1} \cdot k(\delta)\, d\delta}{\int_0^{\pi/2} D_{\delta 1}\, d\delta} = \frac{\int_0^{\pi/2} (\cos\delta + 2\cos^2\delta)\sin\delta\, k(\delta)\, d\delta}{\int_0^{\pi/2} (\cos\delta + 2\cos^2\delta)\sin\delta\, d\delta} \cdots\cdots 7$$

or

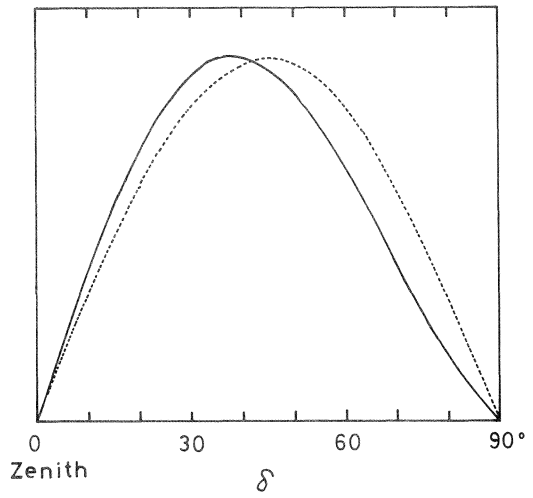

Fig. 14. Angular distribution of diffuse radiation received on a horizontal surface based on the SOC and UOC models. Ordinate is an arbitrary unit. Solid and broken lines indicate the SOC and the UOC models, respectively.

$$RD_2=\frac{\int_0^{\pi/2} D_{\delta 2}\cdot k(\delta)\,\mathrm{d}\delta}{\int_0^{\pi/2} D_{\delta 2}\,\mathrm{d}\delta}=\frac{\int_0^{\pi/2}\cos\delta\sin\delta\,k(\delta)\,\mathrm{d}\delta}{\int_0^{\pi/2}\cos\delta\sin\delta\,\mathrm{d}\delta} \quad \cdots\cdots 8.$$

The degrees are converted to radians in the above equations.
If

$k(\delta)=K=\text{const.}$,

then,

$RD_1=RD_2=K$.

If a radius δ' in the circular hemispherical image corresponds to the zenith angle δ, the proportion of the openings in the image (p) becomes

$$p=\frac{\int_0^R 2\pi\delta' k(\delta')\,\mathrm{d}\delta'}{\int_0^R 2\pi\delta'\,\mathrm{d}\delta'},$$

where R refers to the radius of the hemispherical image corresponding to 90° or $\pi/2$.
If

$k(\delta')=K$,

then,

$$p=\frac{K\pi R^2}{\pi R^2}=K.$$

This means that the proportion of the openings corresponds to the relative diffuse radiation. However, it remains to be determined whether $k(\delta)=K$=const. or not. The radius of the circular image of an *A. auriculiformis* stand was divided into fractions of 10°, and the proportion of the openings was calculated for every 10° (Fig. 15). As shown in the figure, the proportion was not constant throughout each 10°. In general, the openings tended to be concentrated around the zenith in the hemispherical image. In addition, the radiation from low altitude did not contribute significantly to the light climate because of the cosine law. Based on Fig. 14, the opening proportion in the range of 40° to 50° plays a key role in the diffuse radiation received on the ground. These facts imply that a relatively small area around the center of the image is mainly responsible for the light conditions under the canopy. Obviously, the higher the opening proportion, the higher the incident diffuse radiation. The above-mentioned reports showing the presence of a high correlation between the proportion and the RI can account for this fact.

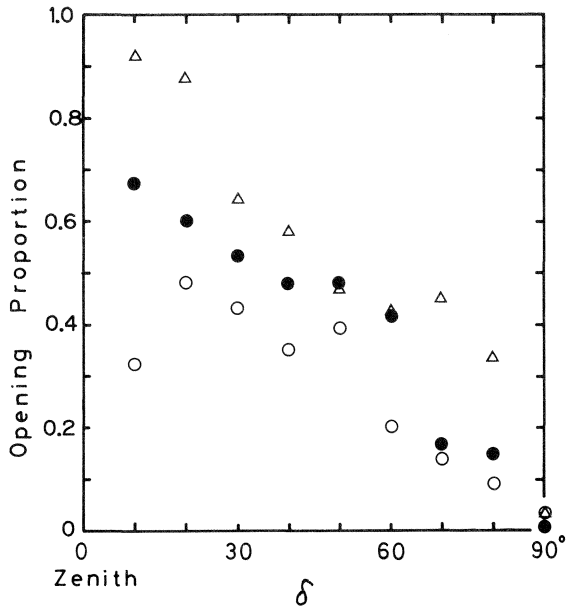

Fig. 15. Opening proportion for every 10° from the zenith in three hemispherical photographs taken in an *Acacia auriculiformis* A. CUNN. ex BENTH. stand. Each series of identical symbols refers to each photograph.

V. Light climate in *Acacia auriculiformis* A. CUNN. ex BENTH. stands of the reforestation project site, Carranglan, Nueva Ecija, Central Luzon

In the reforestation project site in Carranglan, Nueva Ecija, the light climate on the forest floor of *A. auriculiformis* stands was actually analyzed based on instantaneous and cumulative measurements of solar radiation and hemispherical photographs. Diffuse and direct radiations were separately assessed here and both were combined as total radiation. The measurements were carried out in January and February of 1987.

1. Study sites and methods

1) Study sites

The study sites were located in the Central Trial Plantation (CTP) and in Monchitchit (MCC). In CTP, nine points were selected for the instantaneous and seven for the cumulative measurements. On the other hand, the instantaneous sensors and the accumulators were placed on the same seven selected points in MCC. The stand conditions around the measurement points are indicated in Table 3.

Table 3. General description of stands of *Acacia auriculiformis* in study sites in Carranglan

Site		mean DBH (cm)	mean Height (m)	Stand density (ha^{-1}) Stumps	Stems	Year planted
CTP[a] -	1	5.6	4.55	1,061	1,415	
	2	5.3	4.44	884	1,149	
	3	7.3	5.44	2,586	3,183	
	4	5.6	4.74	1,783	2,165	
	5	6.7	5.47	1,528	1,910	1981
	6	5.4	4.62	1,680	1,945	
	7	5.3	4.93	1,655	1,910	
	8	6.7	4.89	1,790	2,188	
	9	5.0	4.88	1,910	2,546	
MCC[b] -	1	6.6	8.46	2,188	3,979	
	2	7.0	8.21	2,387	2,785	1980
	3	12.9	10.74	891	1,146	
	4	6.6	6.81	891	1,655	
	5[c]	-	-	-	-	
	6	3.2	3.49	1,146	1,783	1984
	7	4.8	5.09	1,194	1,790	1983

a) Central Trial Plantation
b) Monchitchit
c) Open field

2) Radiation measurement

The QS type sensor for the photon flux density between 400 and 700 nm and the ES type sensor for the radiant flux density between 400 and 1,000 nm were used for the instantaneous measurements. These sensors were already described in the preceding

chapter. At the same measurement point, a sunstation model C7A was also set for 25 days from Jan. 15 to Feb. 11. This instrument accumulates solar energy during a given period. This sensor is sensitive to the radiation in the range of 350 and 1,100 nm but most sensitive to that of 700 nm.

3) Hemispherical photography

The Fisheye-Nikkor 8 mm f/2.8 lens mounted on the Nikomat FTN type camera was used for photographing the hemispherical image. The image was recorded on Tri-x film ISO 400 for black/white prints. Although the exposure and the shutter speed were determined by the TTL measurement system of the camera, the shutter was clicked at 1/250 second in most cases.

4) Opening proportion in the hemispherical image (r_2)

The enlarged circular image 9 cm in radius was printed for the analysis. The proportion of the openings within the zenith angle 70° in the image was estimated using a transparent plate with dots spaced regularly at 2 mm intervals, and it was designated as r_2 here. There are two reasons for the adoption of 70°. As discussed above, diffuse radiation from low altitude does not contribute significantly to the total one. Another reason is that, the smaller the measurement area becomes, the more easily the proportion can be calculated in the image.

5) Relative direct radiation (r_1)

From the latitude of the measurement point (z), the hour angle of the sun(t), and the sun's declination for the given day(s), the solar altitude(h) and the solar azimuth(q) can be calculated as

$$\sin h = \sin z \sin s + \cos z \cos s \cos t$$

$$\sin q = \frac{\cos s \sin t}{\cos h}$$

The hour angle, being equal to one hour for 15°, becomes negative in the morning, positive in the afternoon, and 0° at noon. By superimposing the solar tracks calculated by the above equations on the hemispherical image in the area in question, it is possible to determine the time when the direct radiation reaches this area and the altitude from which the direct radiation comes or at which it is obstructed by tree components[2)9)12)]. In the meantime, the radiation from the zenith angle δ is proportional to cos δ based on the consine law (Fig. 16). Based on these data and the

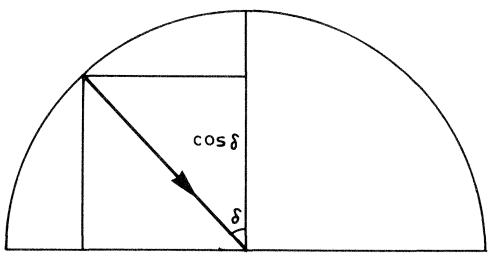

Fig. 16. Simplified illustration of direct solar radiation in relation to the zenith angle δ.

equation $\delta=90°-\theta$, the relative direct radiation reaching the point (r_1) can be defined as

$$r_1 \equiv \frac{\sum_{i=1}^{n} \int_{\beta i}^{\alpha i} \sin\theta \, d\theta}{2\int_{0}^{h} \sin\theta \, d\theta} = \frac{\Sigma(\cos\beta_i - \cos\alpha_i)}{2(1-\cos h)}$$

where h refers to the solar altitude at noon, n the number of openings along the solar track, and α_i and β_i the starting and the ending angle of the i th opening on the track. Here, the sun is regarded as a point and not as a disc.

6) Mean relative distance (M)

As an index of stand structure, the mean relative distance (M) was defined as

$$M \equiv \frac{\sum_{i=1}^{n} \tan\gamma_i}{n} = \frac{\Sigma h_i/d_i}{n},$$

where n refers to the arbitrary number of the nearest trees from the measurement point, γ_i the angle of elevation from the point to the top of the i th tree, h_i the height of the i th tree, and d_i the distance between the i th tree and the measurement point (Fig. 17). Six was adopted as n in this experiment because six was the minimum out of the nearest trees measured at each point. The calculated M at each point will be presented later in Table 4.

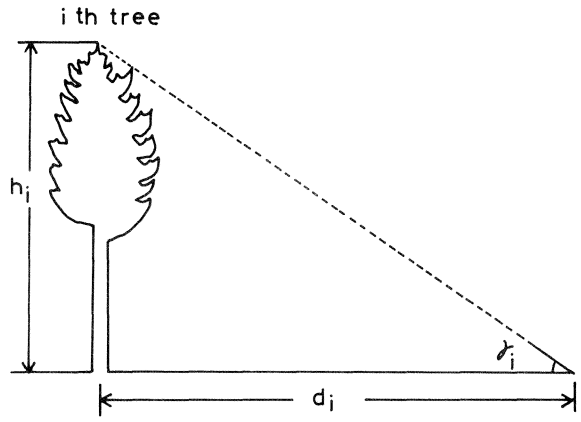

Fig. 17. Diagrammatic representation of h_i, d_i and γ_i in relation to the calculation of M. (Details in the text)

2. Results and discussion

1) Weather conditions during the measurements

The weather conditions in Carranglan from Jan. 15 to Feb. 11 were as follows: 18 clear and 9 cloudy days. However, since the record was made once in the morning each day, clouds on the "cloudy" day might be blown off in the afternoon, and vice versa. No rain was observed as the measurements were performed in the dry season.

2) Measurement of instantaneous diffuse radiation

Even in the same area, solar radiation fluttered for a very short period of time due to the shaking of the crown by the wind. Fluttering caused major fluctuations of the record on the chart. An example of fluctuation is presented in Photo. 2. The pattern of the fluctuation appears to consist of two components, i.e. the almost stable minimum value and the fluctuating values from the minimum. Since the fluttering is attributable to the instantaneous incident direct radiation, the minimum value may reflect the diffuse radiation without the direct one. Therefore, the minimum values will be considered to represent the diffuse radiation.

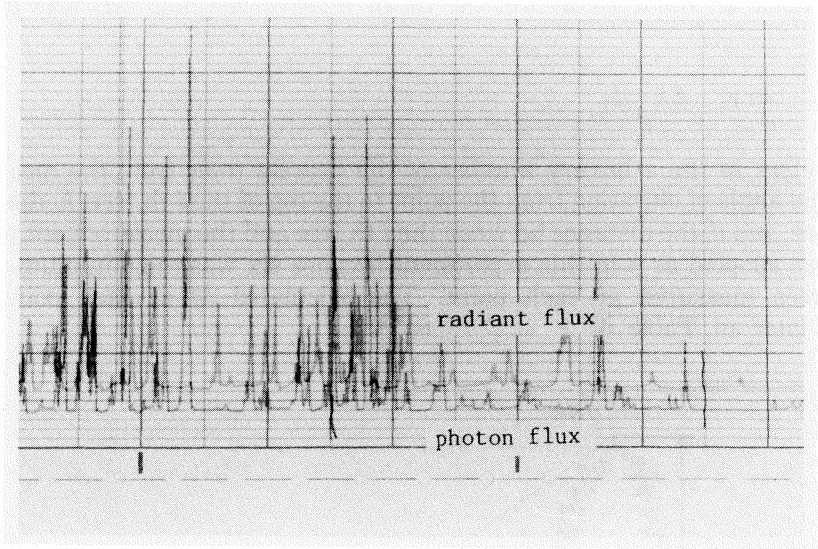

Photo.2. Example of recording chart showing fluctuation of solar radiation by fluttering.

3) Relationship between diffuse radiation under the canopy and r_2

The analysis revealed a high positive correlation, especially for the photon flux density of PAR, between the opening proportion within the zenith angle 70° (r_2) and the diffuse radiation, although scattering was more or less observed (Fig. 18). These findings suggest that the relative values of the diffuse radiation are closely correlated with the opening proportion even within the zenith angle 70°. In the radiant flux density in the range of 400 to 1,000 nm, the decrease in the value with the decrease of the opening proportion was smaller than in the photon flux density in the range of 400 to 700 nm (Fig. 19). As the ES type sensor is sensitive to the infrared zone above 700 nm, this fact may support the observation of the higher percentage of infrared radiation under the leaf layer than outside[14)20)21)].

The difference in the regression lines between CTP and MCC which is indicated in Figs. 18 and 19, may be ascribed to the difference in total diffuse radiation from the sky. Measurement at CTP and MCC was carried out on different days.

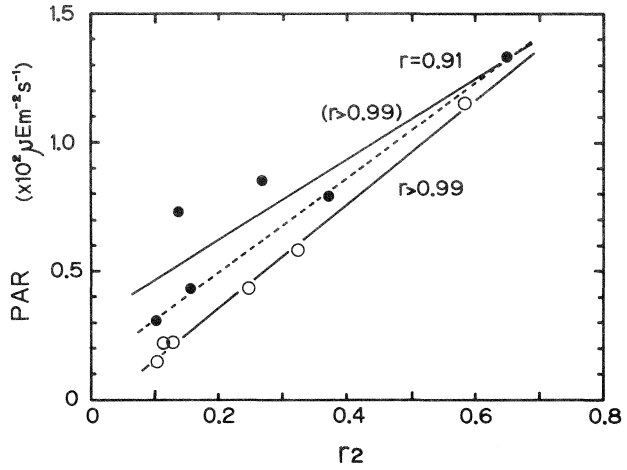

Fig. 18. Correlation for photon flux density of PAR between r_2 within the zenith angle 70° and diffuse radiation. Open and solid circles refer to the data for MCC and CTP, respectively. Solid lines indicate the regression lines for all the data in each stand, and broken line refers to the data excluding those at two sites of CTP.

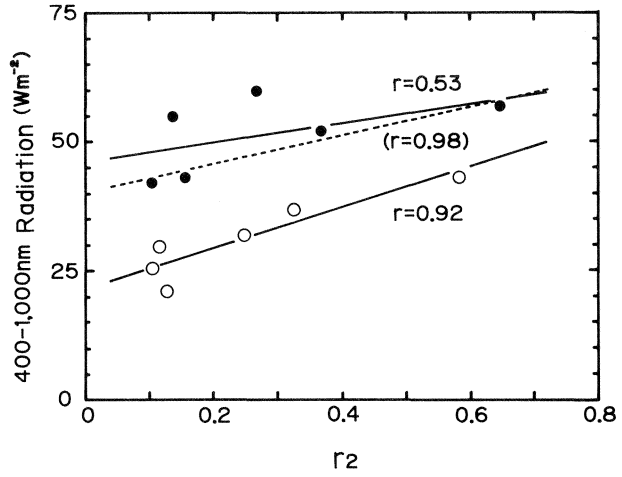

Fig. 19. Correlation for radiant flux density of 400-1,000 nm between r_2 and diffuse radiation. Symbols are the same as in Fig. 18.

4) Daily total solar radiation

When the daily total radiation of a point under the canopy and the daily direct and diffuse radiation in the open are represented as T_d, I_d and D_d, respectively, the T_d can be expressed as

$$T_d = r_1 I_d + r_2 D_d + C$$

This equation is derived based on the following assumptions;

$$I = r_1 I_d + C_1 \quad \cdots\cdots 9$$
$$D = r_2 D_d + C_2 \quad \cdots\cdots 10$$
$$C = C_1 + C_2 \ ,$$

where I and D refer to the direct and diffuse radiation under the canopy. C_1 and C_2 in the equations should be regarded as a correction term for the error caused by the reflection and the transmission of direct and diffuse radiation.

Equation 9 can be derived from the following procedures. The weather varies even during a day, e.g. from clear to cloudy, from rainy to clear, and so on. Based on the weather variations and shaking of tree components by the wind, the time of the day when the direct solar radiation reaches the measurement point can be assumed not to be fixed but rather randomly distributed. Hence, the direct solar radiation under the canopy may be approximated by equation 9.

It was previously stated that r_2 was closely proportional to the instantaneous diffuse radiation. We applied this direct proportion to the relationship between accumulated diffuse radiation and r_2 represented by equation 10.

5) Total solar radiation reaching the ground during a certain period

Let the total accumulated solar energy for a certain period be T, then,

$$T = r_1 \Sigma I_d + r_2 \Sigma D_d + \Sigma C \quad \cdots\cdots 11$$

on the assumption that there is no change in r_1 and r_2 during that period. this equation agrees with that proposed by ANDERSON[2], and also fits to the multiple regression model.

Fourteen sunstations in total were set up at various points of *A. auriculiformis* stands, and hemispherical photographs were taken at each point. The T, r_1 and r_2 values at each point can be obtained based on the location of the sunstations and on the hemispherical photographs. If ΣI_d, ΣD_d and ΣC are common to all the points in that region, the following equations can be derived;

$$T_1 = r_{11} \Sigma I_d + r_{21} \Sigma D_d + \Sigma C$$
$$T_2 = r_{12} \Sigma I_d + r_{22} \Sigma D_d + \Sigma C$$
$$\vdots$$
$$T_n = r_{1n} \Sigma I_d + r_{2n} \Sigma D_d + \Sigma C$$

where T_n, r_{1n}, and r_{2n} refer to T, r_1 and r_2 at the n th point, respectively. The ΣI_d, ΣD_d and ΣC can be estimated by the least squares method, because the ΣI_d and ΣD_d were never measured separately. The r_2 and r_1 values at each point were calculated from the hemispherical photographs taken on Feb. 11 and by superimposing the solar track on Jan. 29 on the image, respectively. Only one solar track on Jan. 29 was used for the

analysis here due to the short measurement period and possible reading errors, although the sun follows a different track every day. T, r_1 and r_2 at each point are presented in Table 4 together with M.

Table 4. T[a], r_1, r_2, and M of stand in each study site

Site	T (KWhm^{-1})	r_1	r_2	M
CTP - 1	40.60	0.518	0.649	1.292
2	79.71	0.885	0.948	0.644
3	20.25	0.218	0.102	3.425
4	38.90	0.389	0.371	2.020
5	20.04	0.167	0.135	1.965
8	24.21	0.238	0.156	2.994
9	56.26	0.424	0.447	1.546
MOC - 1	15.87	0.086	0.116	3.460
2	16.47	0.123	0.102	4.717
3	16.85	0.157	0.130	2.874
4	40.59	0.437	0.249	2.128
5	79.41	0.975	0.998	-
6	68.75	0.624	0.585	1.493
7	40.50	0.198	0.323	1.815

a) T was measured by the sunstation system, which integrates solar radiation absorbed during the period Jan. 15 and Feb. 10, 1987. During this period there were 18 clear and 9 cloudy days, including Jan. 15, respectively. The sunstation system was not used at CTP-6 and 7.

The estimates of ΣI_d, ΣD_d and ΣC are shown in the following equation, by which the total solar energy reaching any point of the *A. auriculiformis* stand from Jan. 15 to Feb. 11, 1987, could be calculated;

$$T=63.86r_1+14.92r_2+9.40 \quad \cdots\cdots 12$$

The unit of T is KWhm^{-2}.

In Fig. 20, the residuals of the estimates by equation 12 are diagrammatically represented in relation to r_1, r_2 and T. They are almost evenly distributed despite the considerable scattering. Judging from the accuracy of the instruments and the reading error of the hemispherical images, it is considered that equation 12 can be applied to estimate the total solar energy at a point during that period in Carranglan.

6) Total radiation in relation to M, r_1 and r_2

Several approximations were made for the relationship between M and r_1 and r_2 as follows;

$$r_n=aM+b \quad \cdots\cdots A_1$$

$$r_n=a\log M+b \quad \cdots\cdots A_2$$

$$\log r_n=aM+b \quad \cdots\cdots A_3$$

$$\log r_n=a\log M+b \quad \cdots\cdots A_4$$

$$\frac{1}{r_n}=\frac{1}{e^b M^a}+1$$

or $\quad \cdots\cdots A_5$

$$\log\left(\frac{1}{r_n}-1\right)=-a\log M-b\ ,$$

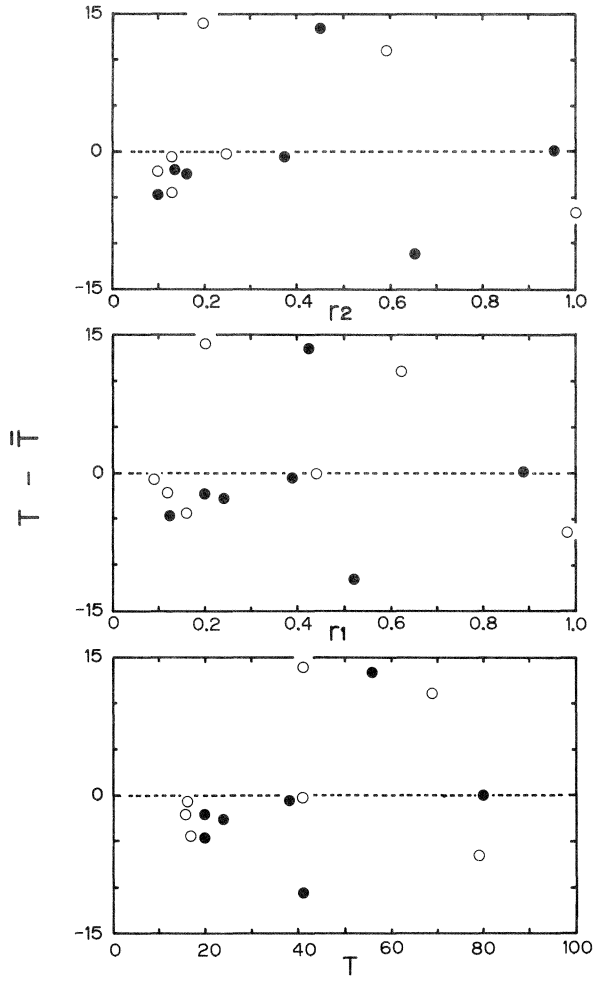

Fig. 20. Scattering diagram of residuals (T-$\bar{T}$) against r_2, r_1 and T. $\bar{T}$ is the estimate.

where a and b refer to the regression coefficients, and the subscript n of r_n indicates 1 or 2. The correlation coefficient and the regression coefficients a and b of each approximation are listed in Table 5. For both r_1 and r_2, the highest correlation was found in the equation A_5, the form of which is called the generalized allometric function[19]. From this equation,

$$\lim_{M\to 0} r_n = 1 \quad \text{and} \quad \lim_{M\to \infty} r_n = 0$$

Hence, the r_n values can be found between 1 and 0, indicating that equation A_5 would be more suitable than the other equations. Figs. 21 and 22 show the relationship between r_n and M and the curve drawn using the approximation by A_5.

By the introduction of the r_n - M approximation to equation 12, the following equation is obtained;

Table 5. Approximations of the relationship between r_1 or r_2 and M

[15 samples]

	Approximation	r_1			r_2		
		a	b	r[a)]	a	b	r[a)]
A_1	$r_n=aM+b$[b)]	-0.1652	0.7288	-0.8065	-0.1949	0.7803	-0.8227
A_2	$r_n=a\log M+b$	-0.3919	0.6314	-0.9002	-0.4690	0.6700	-0.9315
A_3	$\log r_n=aM+b$	-0.5157	-0.0551	-0.8425	-0.6258	0.0785	-0.8921
A_4	$\log r_n=a\log M+b$	-1.1241	-0.4283	-0.8638	-1.3817	-0.3621	-0.9265
A_5	$\log\left(\frac{1}{r_n}-1\right)=-a\log M-b$ or $\frac{1}{r_n}=\frac{1}{e^b M^a}+1$	-2.0121	0.7248	0.9034	-2.6182	1.0696	0.9426

a) Correlation coefficient
b) n of r_n refers to 1 or 2.

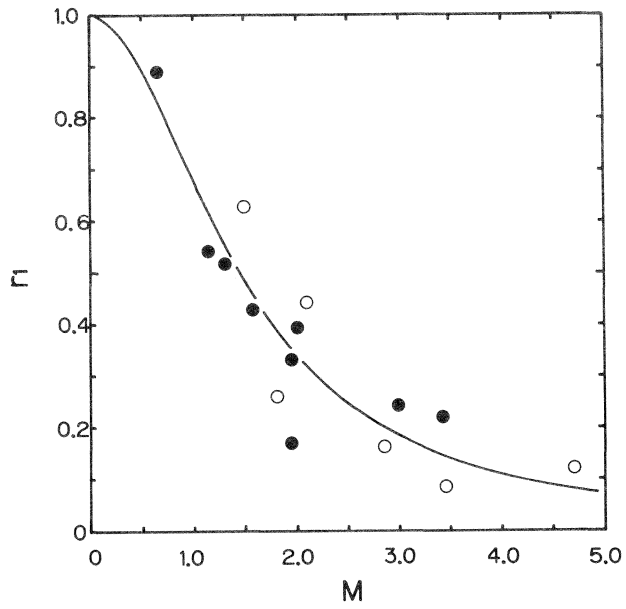

Fig. 21. Relationship between r_1 and M in CTP and MCC. The curve was approximated using equation A_5. Open and solid circles refer to the MCC and CTP sites, respectively.

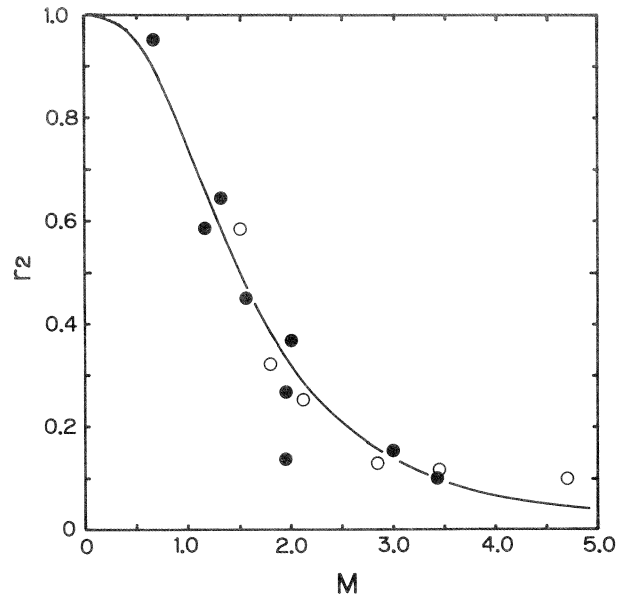

Fig. 22. Relationship between r_2 and M in CTP and MCC. Symbols are the same as in Fig. 21. The curve was approximated by equation A_5.

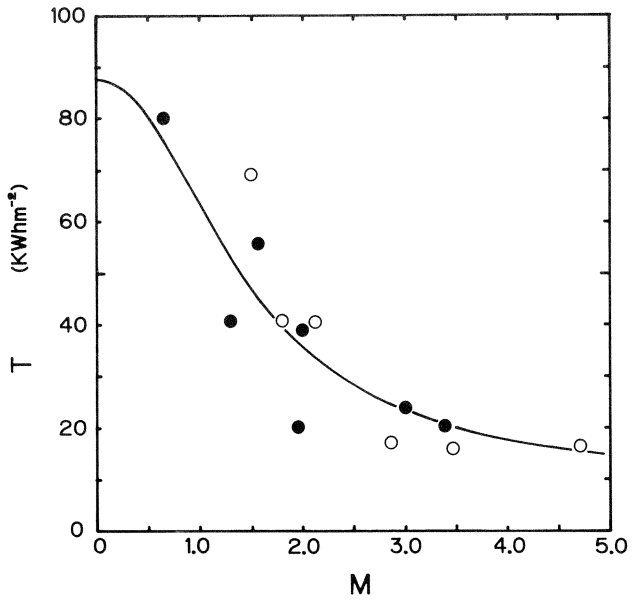

Fig. 23. Relationship between T and M in CTP and MCC. Symbols are the same as in Fig. 21.

$$T=63.86\times\frac{1}{0.4844M^{2.0121}+1}+14.92\times\frac{1}{0.3431M^{2.6182}+1}+9.40\cdots\cdots\cdots 13.$$

When T_0=63.86+14.92+9.40=88.18,
the *relative* $T(T/T_0)$ is

$$\frac{T}{T_0}=\frac{1}{88.18}\times T \cdots\cdots 14.$$

In Fig. 23, T is given in relation to M. The curve in the figure was drawn based on equation 13. Although there is considerable scatttering, the curve appears to follow the general trend. The *relative* T at that point could be roughly estimated from equations 13 and 14 (Fig. 24), although the period was limited to January and February in this case.

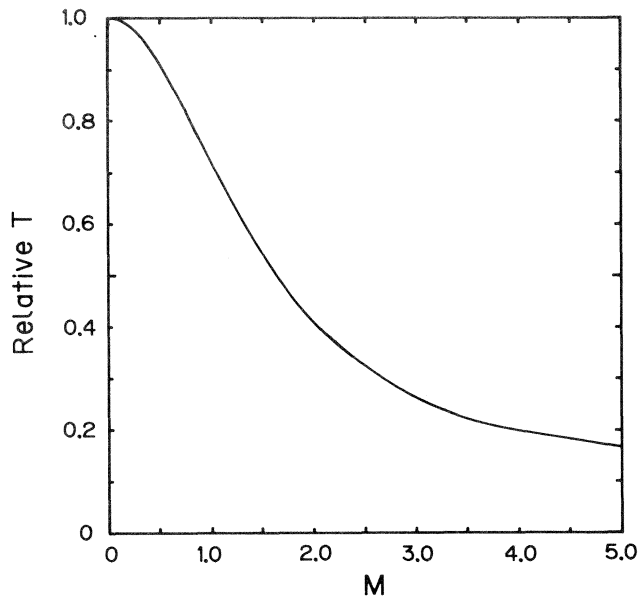

Fig. 24. Approximation of the relationship between *relative T* and *M* on the basis of equation A_5.

7) Changes in relative total solar radiation on the ground (*relative T*) with increasing tree height

The changes in the relative total solar radiation on the floor (*relative T*) with increasing tree height were simulated using the same data for the *A. auriculiformis* stands based on equations 13 and 14. Let four points *a, b, c,* and *d* be arranged as shown in Fig. 25 between rows of the trees planted at a spacing of 2 × 2 and 2 × 4 m. Then, it is easy to measure the distance between the points and each position of the nearest six trees. The distance to the nearest trees becomes equal for points *b* and *d*. On the assumption that the six trees have the same height, M can be easily calculated at each tree height of 2, 4, 6, and 8m. Hence, the *relative T* at the M can be deduced from equations 13 and 14. Fig. 26 can be drawn by linking the *relative T* at each tree height

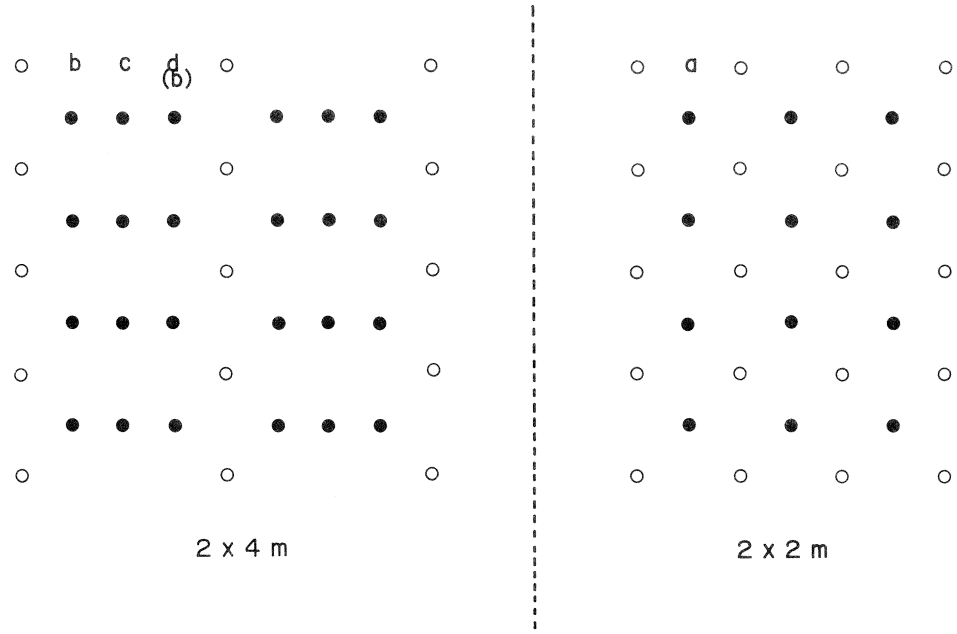

Fig. 25. Hypothetical arrangement patterns of trees (open circles) spaced at 2×4 m and 2×2 m, and several points of *a, b, c* and *d* (solid circles) between the trees. Vertical and horizontal rows of trees and points are set at an interval of 1 m.

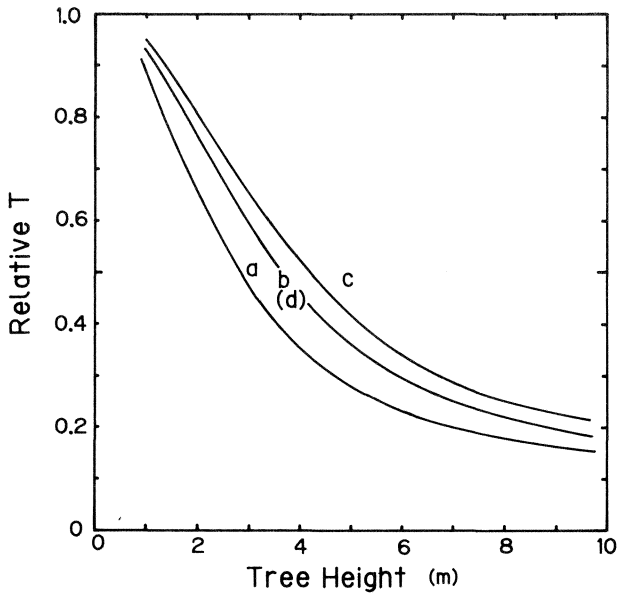

Fig. 26. Changes in *relative T* at points *a, b*(*d*) and *c* with the change of tree height. The position of the points is diagrammatically represented in Fig. 25.

for each point.

Silvicultural practices applied to the stand to obtain an objective *relative T* would become possible based on the diagram of Fig. 26. For example, suppose that the *relative T* at point *a* is maintained at 0.4. According to the diagram, the *relative T* at that point becomes 0.4 when the tree height is 3.5 m. If no silvicultural practices are applied to the stand at that stage the value of the *relative T* decreases. If thinning is practiced, the value of M decreases because the distance to the nearest six trees become longer after thinning than before even at the same height. The decrease in the M value is effective in increasing the *relative T* value. As field crops and seedlings need usually strong solar radiation, the *relative T* should be also strong. The diagram shown in Fig. 26 would be useful to control the *relative T* and to get strong radiation by thinning or other practices. However, this diagram is valid only for the period from January and February. In addition, the change in the regression coefficients between r_1 or r_2 and M by the change in the tree form through thinning, pruning and other practices may create problems. Further studies will be needed for the improvement of the diagram in considering seasonal changes in radiation, changes in the tree form associated with silvicultural practices, differences in species, and so on.

VI. General discussion

In the Philippines, the most popular multistoried agroforestry systems consist of various combinations of coconut palm (*Cocos nusifera* L.) with other agricultural crops. Typical patterns include the combination of coconut palm — banana (*Musa* spp.), coconut palm — coffee (*Coffea robusta* LINDEN), and coconut palm — pineapple (*Ananas comosus* MERR.). Coconut palm never falls under the category of trees. Instead of coconut palms, attempts are made at planting tree species as an upper layer component from the viewpoint of forestry. For example, a related government organization recommends combinations of pines (*Pinus khasya* ROYLE) with coffee and ipil-ipil (*Leucaena leucocephala* DE WIT), a nitrogen-fixing and fast-growing species, with annual or perennial crops. In the case of pine, the recommended spacing is 3m between the trees with coffee planted at a 4m height from the pines[1].

Since coconut palms appear to require much space for nut production, the agroforestry system using this species may have originated probably from the cultivation of vacant ground between coconut palms to promote a more efficient land use. The main reason for the success of this system is that the available radiation reaching the ground is high enough for growing crops there. Since this palm has a small crown without branches and the crown position increases in height with the progression of growth, more radiation must be received on the floor as compared with trees, for an identical spacing. Undoubtedly solar radiation is important for growing crops. In Thailand, KANAZAWA observed a *Melia azedarach* L. plantation pruned by farmers to let more radiation reach the ground for the growth of cassava (*Manihot esculenta* CRANTZ). Since coffee trees require a certain amount of shade, they can be easily cultivated as a lower crop in a multistoried agroforestry system. On the other hand, the selection of upper layer species involving spacing and tending should be carefully considered for light-demanding lower crops such as pineapples and bananas.

Hemispherical photographs of two stands in a coconut plantation were taken where coffee and pineapples were the lower crops, respectively, and the relative direct radiation (r_1) described above as well as the proportion of openings (r_2), and the mean relative distance (M) of both stands were determined. The possibility of developing a multistoried agroforestry system using *A. auriculiformis* was evaluated based on the results of the experiments previously reported as the data on the coconut plantation. Unfortunately, actual radiation was not measured in the coconut stands. The values of r_1, r_2, and M are presented in Table 6. In this case, r_1 was estimated annually, and r_2 was calculated within a zenith angle of 90° instead of 70°.

Table 6. r_1[a], r_2[b] and M in two stands of a multistoried coconut palm (*Cocos nucifera* L.) plantation

Spacing	M	r_1	r_2	Lower crop
ca. 10×10 m	1.6	0.57	0.42	Pineapple (*Ananas comosus* MERR.)
ca. 10×10 m	1.9	0.54	0.34	Robusta coffee (*Coffea robusta* LINDEN)

a) Annually estimated value
b) Estimated from a whole hemispherical image

According to Table 6, M value of *A. auriculiformis* should be kept at 1.5 - 1.8 to maintain a r_2 of 0.34 or 0.42, and r_1 of 0.54 or 0.57 for the cultivation of pineapples or coffee, (Figs. 21 and 22) although the calculation base was different. As a coconut palm has a smaller crown and higher crown height, the r_1 and r_2 values for a plantation are presumably higher than those for a plantation of *A. auriculiformis* even if the same M value is observed. This means that the spacing of *A. auriculiformis* trees should be wider than that of coconut palms.

The available radiation for the production of the lower crops can be controlled by the spacing of the upper layer trees. The conditions of openings in the canopy necessary for growing lower crops can be determined by analyzing the hemispherical image of the existing system. The conditions can probably be met by modifying the spacing of the upper layer component through planting and cutting. Before the establishment of a desirable combination of crops, however, the characteristics of the upper layer component which influence the conditions in the canopy should be determined.

As mentioned above, the proportion of direct solar radiation out of the total radiation reaching the ground is higher than that of diffuse radiation. Since the amount of direct radiation is determined by the solar altitude and orientation, the amount of direct radiation received on the forest floor is likely to be affected by the orientation of rows of trees and their spacing. It may be possible to intercept direct radiation due to the inter-relationships between the orientation of the rows of trees, distance between them, and tree height. In the high latitudinal region, these factors may affect appreciably the seasonal changes in the light climate on the ground, because seasonal solar tracks show more pronounced variations than in the low latitudinal region, e.g. in the tropics. Their effects on the radiation climate for lower layer crops should be compared between the two regions.

The period of measurement under the canopy of the *A. auriculiformis* stand was limited to approximately one month of the year, although changes in the light climate and stand structure and their interaction should have been followed throughout a year as HUTCHISON & MATT did[13]. In addition, the analysis of the relationship between the light or radiation climate and stand structure should be undertaken with more accuracy. Furthermore, there are still several important factors which should be analyzed such as the light quality in the plant community which affects the morphogenesis of plants[10)23)], and penumbral effects of the sun in canopies[5)10)22)].

VII. Summary

Since, in a multistoried agroforestry system, trees and agricultural crops or seedlings are simultaneously cultivated in the upper and lower layers, respectively, the growth of the lower component is greatly affected by the light condition created by the upper layer. Hence, the light climate under the canopy was analyzed in this report. The results are as follows.

Illuminance under the tree crown was proportional to that in the open within a certain range. But when the latter exceeded the range, the former rather decreased. This could be attributed to the lack of discrimination of the measurements between the direct and diffuse fraction of the light. Both fractions should be assessed separately.

Model experiments of shading by changing opening angles above the horizon demonstrated that photon or radiant flux density under the shade tended to be more or less stable despite the large fluctuations in the open. The stable value depended on the total diffuse radiation from the sky and the opening angle. Diffuse radiation from the sky could be roughly approximated by two models of the standard overcast sky (SOC) and the uniform overcast sky (UOC) whether clear or cloudy.

The opening proportion in the hemispherical photographs was closely related to the relative diffuse radiation. An example in an *Acacia auriculiformis* A. CUNN. ex BENTH. stand showed a high correlation even with the opening proportion within the zenith angle 70°.

Actual light climate under the canopy was analyzed for more than ten sites of *A. auriculiformis* stands in Carranglan, Central Luzon, using hemispherical photographs and radiation measurements. Relative value of direct radiation and the opening proportion could be estimated from the hemispherical photographs. Based on these data and the radiation measurement, the relationship between stand structure and total radiation received at the site for a given period could be formulated, and the change in the relative total radiation there could be diagrammatically illustrated with the height growth of trees around the site. An example illustrating how to control the relative total radiation was presented using this diagram.

The results obtained for *A. auriculiformis* stands were compared with those obtained in preliminary studies of actual multistoried systems of coconut palms and other agricultural crops, and the possibility of using *A. auriculiformis* as a system was considered.

References

1) Agroforestry Committee (1986): The Philippines recommends for agroforestry. PCARRD Technical Bulletin Series No. 59 PCARRD, Los Baños, Laguna, Philippines, 90pp.
2) ANDERSON, M.C. (1964): Studies of the woodland light climate I. The photographic computation of light conditions. *J. Ecol.*, **52**, 27-41.
3) ———— (1964): Ditto II. Seasonal variation in the light climate, *Ibid.*, **52**, 643-663.
4) ———— (1970): Interpreting the fraction of solar radiation available in forest. *Agr. Meteorol.*, **7**, 19-28.
5) ———— and MILLER, E.E. (1974): Forest cover as a solar camera: Penumbral effects in plant canopies. *J. appl. Ecol.*, **11**, 691-698.
6) ANDO, T. (1983): Measurement of openness grade of canopy by hemispherical photograph. *Bull. For. & For. Prod. Res. Inst.*, **323**, 4-8. (in Japanese).
7) CHAN, S.S., MCCREIGHT, R.W., WALSTAD, J.D. and SPIES, T.A. (1986): Evaluating forest vegetative cover with computerized analysis of fisheye photographs. *Forest Sci.*, **32**, 1085-1091.
8) CHANDLER, T. and SPURGEON, D. (1979): International cooperation in agroforestry. ICRAF, DSE, Nairobi, Kenya, 469pp.
9) EVANS, G.C. and COOMBE, D.E. (1958): Hemispherical and woodland canopy photography and the light climate. *J. Ecol.*, **47**, 103-113.
10) ———— (1966): Model and measurement in the study of woodland light climate. In "Light as an ecological factor (BAINBRIDGE, R., EVANS, G.C. and RACKHAM, O. eds.)", Blackwell Scientific Publications, Oxford, U.K., 452pp. [ref. 53-76]
11) ————, FREEMAN, P. and RACKHAM, O. (1975): Developments in hemispherical photography. In "Light as an ecological factor II (EVANS, G.C., BAINBRIDGE, R. and RACKHAM, O. eds.)". Blackwell Scientific Publications, Oxford, U.K., 616pp. [ref. 549-556]
12) HOLBO, H.R., CHILDS, S.W. and MCNABB, D.H. (1985): Solar radiation at seedling sites below partial canopies. *For. Ecol. and Manage.*, **10**, 115-124.
13) HUTCHISON, B.A. and MATT, D.R. (1977): The distribution of solar radiation within a deciduous forest. *Ecol. Monog.*, **47**, 185-207.
14) KUMURA, A. (1969): Studies on dry matter production of soybean plant VI. Changes in spectral composition of solar radiation penetrating through leaf canopy and photosynthetic rate of single leaf as affectd by light quality. *Proc. Crop Sci. Soc. Jap.*, **38**, 408-418. (in Japanese with English summary)
15) MADGWICK, H.A.I. and BRUMFIELD, G.L. (1969): The use of hemispherical photographs to assess light climate in the forest. *J. Ecol.*, **57**, 537-542.
16) MONSI, M. und SAEKI, T. (1953): Über den Lichtfaktor in den Pflanzengesellschaften und seine Bedeutung für die Stoffproduktion. *Jap. J. Bot.*, **14**, 22-52.
17) MONTEITH, J.L. (1973): Principles of environmental physics. Edward Arnold (Publishers) Limited, London, U.K., 241pp.
18) NAIR, P.K.R. (1980): Agroforestry species. ICRAF, Nairobi, Kenya, 336pp.
19) OGAWA, H., YODA, K., OGINO, K. and KIRA, T. (1965): Comparative ecological studies on the three main types of forest vegetation in Thailand II. Plant biomass.

Nat. & Life in SE Asia, **4**, 49-80.
20) PROCTOR, J.T.A., KYLE, W.J. and DAVIES, J.A. (1975): The penetration of global solar radiation into apple trees. *J. Amer. Soc. Hort. Sci.,* **100**, 40-44.
21) ROBERTSON, G.W. (1966): The light composition of solar and sky spectra available to plants. *Ecology,* **47**, 640-643.
22) SAEKI, T. (1973): [Light climate and dry matter production] (tentative translation by the present authors). *KAGAKU,* **43**, 635-638. (in Japanese)
23) SASAKI, S. and MORI, T. (1981): Growth responses of dipterocarp seedlings to light. *Malaysian Forester,* **44**, 319-345.
24) SUZUKI, T. and SATOO, T. (1954): An attempt to measure the daylight-factor under crown canopy with the solid angle projecting camera. *Bull. Tokyo Univ. For.,* **46**, 169-180. (in Japanese with English summary)
25) TAMAI, S. and SHIDEI, T. (1972): Light intensity in the forest I. *Bull. Kyoto Univ. For.,* **43**, 53-62. (in Japanese with English summary)
26) ———— and ———— (1972): Ditto II. The hemispherical photographic computation of light intensity I. *Ibid.,* **44**, 100-109. (in Japanese with English summary)
27) WASEDA, O. (1983): Measurement of openness grade of canopy and application for the index of light condition. *Bull. For. & For. Prod. Res. Inst.,* **323**, 9-13. (in Japanese)

熱帯地方植栽林の林床光環境解析

金沢洋一*,**・中村松三***・Roberto V. DALMACTO****

摘要

上層に林木、林床に作物などを栽培する複層構造のアグロフォレストリーを想定し、下層の植物の成長に大きく影響する光要因を取り上げ、上層の林木によって作り出される林床の光環境について解析を進めた。

樹冠下の照度は、開放地の照度とある範囲ではほぼ比例するが、開放地の照度がその範囲を越えるとむしろ小さくなった。これは、散乱光と直達光を一緒にしたことにより生じたためで、両者を分けて評価する必要があると考えた。

モデルを使って開空角度を変えた被陰試験から、被陰下の日射量および光量子数は、開放地でそれらが大きく変動しても、10分程度の短時間ではほぼ定常状態を示した。その値は直達日射量を除く全天からの散乱日射量あるいは光量子数に依存していた。

全天からの散乱日射量は、曇天、晴天に関係なく、標準的な曇天（SOC）あるいは一様な曇天（UOC）からの入射光モデルでおよそ表現できた。全天写真の開空率と相対散乱日射量には密接な関係がみられ、*Acacia auriculiformis* 林の例では、天頂角70°以内の開空率でも、相対散乱日射量と高い相関があった。

ルソン島中部カラングランの *A. auriculiformis* 林では実際の林床の光環境を調べた。全天写真から相対直達日射量と開空率を推定し、それと実際に測定した日射量から、林分の構造とその林床の日射量の関係を数式化した。この数式にもとづいて、樹高成長に伴う林床の相対全日射量の変化を図示し、その日射量をコントロールする一例を示した。

A. auriculiformis 林で得られた結果と一般にみられるココナツヤシを上層にもつアグロフォレストリーを比較し、*A. auriculiformis* を上層にするアグロフォレストリーの可能性を検討した。

---

*熱帯農業研究センター、**現住所：森林総合研究所北海道支所、
森林総合研究所九州支所、*フィリッピン大学林学部